Electrical-Driven Transport of Endohedral Fullerene Encapsulating a Single Water Molecule

Baoxing Xu and Xi Chen

Phys. Rev. Lett. **110**, 156103 — Published 12 April 2013

DOI: 10.1103/PhysRevLett.110.156103

Electrical-driven Transport of Endohedral Fullerene Encapsulating a Single Water Molecule

Baoxing Xu [a] and Xi Chen [a,b,c *]

[a] *Columbia Nanomechanics Research Center, Department of Earth and Environmental Engineering, Columbia University, New York, NY 10027, USA*

[b] *International Center for Applied Mechanics, SV Lab, School of Aerospace, Xi'an Jiaotong University,*

Xi'an 710049, China

[c] *Department of Civil & Environmental Engineering, Hanyang University,*

Seoul, 133-791, Korea

Abstract:

Encapsulating a single water molecule inside an endohedral fullerene provides an opportunity for manipulating the H_2O@C60 through the encapsulated polar H_2O molecule. Using molecular dynamic (MD) simulations, we propose a strategy of electrical-driven transport of H_2O@C60 inside a channel, underpinned by the unique behavior of water molecule free from hydrogen-bonding environment. When an external electrical field is applied along the channel's axial direction, steady-state transport of H_2O@C60 can be reached. The transport direction and rate depend on the applied electric intensity as well as the polar orientation of the encapsulated H_2O molecule.

Keywords: Endohedral fullerene; Single water molecule; Polar orientation; Transport; Electrical field

Trapping a single atom or molecule inside the hollow interior of a fullerene such as C60 has drawn significant attention because of its unique closed-cage structure and unconventional property[1-5]. The synthesized endohedral fullerene provides a rich and fascinating platform inside which a single atom or molecule may be placed, and the isolated status of the molecule and its

[*] Corresponding author, xichen@columbia.edu

"communication" with the surrounding environment may lead to interesting characteristics and novel functionalities.[6, 7] For example, the pure C60 itself does not have a dipole; whereas H_2O@C60 is a polar molecule due to the high dipole moment of the encapsulated H_2O molecule.[8] The introduction of dipole moment provides a possibility for manipulating C60 through the encapsulated H_2O molecule. On the other hand, many fascinating properties of nanoconfined water, such as unusual phase transition[9, 10] and enhanced transport rate[11-14], are dominated by the pervasive hydrogen bonds. Thus, the possibility of isolating a single molecule of H_2O into the C60 cage opens a door to reveal the intrinsic properties of the single water molecule free from any hydrogen-bonding environment. Using molecular dynamics (MD) simulations, we propose herein (for the first time to the best of our knowledge) a *controllable transport mechanism of H_2O@C60* in a channel, where the motion of the encapsulated H_2O molecule is driven by an external electrical field.

Since the encapsulated H_2O molecule does not affect the structure of the outer C60 cage (See Figures S1a and S1b), this is also consistent with results from *ab* initio MD by Bucher[15], and thus the C60 is assumed rigid here. The water molecule is modeled by the most popular extended simple point charge (SPC/E) potential[16]. The 12-6 pairwise L-J potential and Coulomb interaction are used to model the water-water interaction and carbon-water interaction (see the supplementary materials for the detailed force field and L-J parameters). A single water molecule is placed inside the C60. After equilibrium at temperature of 300K and 1 atm, the oxygen atom of the encapsulated H_2O molecule is located at the center of the C60 cage (See Figure S1c), consistent with the experimental observation[8]. A segment of smooth carbon nanotube (CNT), which has a linear structure and slippery surface,[17] is employed as a channel inside which the H_2O@C60 transports. The radius of the CNT (4.1nm) is chosen to be large enough in comparison with the size of H_2O@C60 (outer radius: 0.5 nm; inner radius: 0.175nm) so as to minimize the effect of CNT wall. The CNT channel is assumed rigid and kept fixed throughout simulation; and its length (19.5nm) is confirmed to be long enough for robust numerical results. Periodical boundary condition is imposed in the axial direction of the computational cell so as to mimic an infinite long channel. The H_2O@C60 is placed into the CNT channel and equilibrated for a period of time t_0 (see Figure S2). An external electrical field, E, is then imposed in the axial direction of CNT channel (i.e. $+z$-direction). We should note that the C60 cage behaves like

a set of separate carbon atoms in a static electric field, and will not fully screen out the external electric field[18]. Additional MD simulation (with the dielectric constant ε (=4.5)[19], using LAMMPS with the NVT ensemble, at 300K by using the Nose/Hoover thermostat [20]) and density functional theory (DFT) calculations are carried out to confirm the relatively minor role of screening effect, see supplementary material.

Regardless of the magnitude of the applied electrical intensity, the H_2O@C60 always transport along the axis of tube (see movie MS1). For C60, only translation is observed and there is no rotational motion during transport; meanwhile, for water molecule, the oxygen atom follows the transport trajectory, yet the H_2O molecule keeps rotating itself which is analyzed below. Under a smaller electrical intensity, e.g. E=0.02 V/Å, the H_2O@C60 transports along the opposite direction of the applied electrical direction (i.e. -z-direction), and the snapshots from MD simulations are given in Figure 1a. Figure 1b presents the transport history of H_2O@C60 along the z-direction and a constant axial transport rate is observed, which demonstrates that an external electrical field may drive the motion of H_2O@C60 in a stable manner, similar to a nanofluidic electroactuation system[21]. When the screening effect of C60 is considered, the stable transport manner will not change (See Figure S3), and this is also confirmed by DFT dynamic calculations (See Figure S11). Note that at a larger electrical intensity, the steady transport direction may be aligned in the same direction with the electrical field (i.e. +z-direction), as shown in Figure S4b and the movie MS2 under E= 0.1V/Å. In the current study, such an inversion of transport direction happens at 0.065V/Å.

To reveal more transport details of H_2O@C60, the polar orientation of the encapsulated H_2O molecule is investigated, whose instantaneous inclination angle θ_t (Figure2a) with regard to the electrical field direction (i.e. +z) is given in Figure 2a, with $\theta_t = \cos^{-1}\left(p_t \frac{\hat{\mu}}{|p_t|} \right)$.[22] Here, $\hat{\mu}$ is a unit vector along +z, t represents a time instant, and p_t is the instantaneous dipole of the H_2O molecule pointing from the H shell to the O shell. During equilibrium and before the electrical field is applied ($t \le t_0$), θ_t fluctuates randomly (Figure 2b). After an electrical field is applied at t_0, θ_t quickly becomes stable – such a steady-state value of the inclination angle of polar orientation of H_2O is referred as θ_{ts}. Figure 2b shows that in the case of E=0.02 V/Å

($t_0 = 0.055ns$), θ_{ts} keeps 68.9° after about $t = 0.1ns$, consistent with the constant axial transport rate of H_2O@C60 (Figure 2a).

Because of the random rotation of H_2O molecule during equilibrium, the inclination angle at the beginning instant of application of electric field, $\theta_0 = \theta_{t=t_0}$, is also random. Nevertheless, Figure 3a shows that the steady-state θ_{ts} is independent of θ_0. That is, after the electric field is applied, the steady-state polar orientation "axis" of H_2O, θ_{ts}, depends only on the magnitude of *E*. Generally, a stronger electrical field tends to align the dipole closer to the direction of the electrical field, leading to a smaller θ_{ts} during transport, which is consistent with present simulation (see Figure S5). Series of simulations show that when θ_{ts} is beyond a critical value (i.e. if the electrical field is not strong enough), there is no stable axial transport of H_2O@C60, referred as unstable state here. Based on the one-to-one correspondence between *E* and θ_{ts}, a map of electric field-driven transport status of H_2O@C60 is plotted in Figure 4, where the axial transport of H_2O@C60 is along the -*z*-direction in region I ($26.7^{\circ} < |\theta_{ts}| < 82.6^{\circ}$ and 0.006V/Å $< E <$ 0.065V/Å), along the +*z*-direction in region II ($0 \le |\theta_{ts}| \le 26.7^{\circ}$ and $E \ge 0.065$V/Å), and unstable in region III ($0 \le E \le 0.006$V/Å) (i.e. flips randomly in the channel). During the stable translational motion of H_2O@C60, in addition to the translational motion (which is coordinated with the C_{60} cage), the encapsulated H_2O molecule also rotates around the axis of the electrical field, resulting in a circular trajectory in the projection plane perpendicular to the electrical direction (See the supplementary material).

The transport rate is investigated next. Figure 3b shows the effect of θ_0 on the transport trajectory of H_2O@C60 along the *z*-direction. Although the steady-state θ_{ts} is independent of θ_0, here the steady-state transport rate, v_{ts}, changes with θ_0, and a higher θ_0 results in a smaller v_{ts}. Conceptually, the electric work required to change the single H_2O molecule from a random θ_0 to a steady θ_{ts} is $pE|\theta_0 - \theta_{ts}|\sin\theta_0$, where *p* is the dipole moment of H_2O molecule ($\sim 6.2\times10^{-30} C\cdot m$ for SPC/E model[23]). Thus, a higher θ_0 will need a larger electrical work, leading to a faster transport rate.

To understand the rotational motions of the encapsulated single H_2O inside C60 and the induced net translational motion of H_2O@C60 along the direction of electric field, we analyze the autocorrelation functions of velocity (*v*-ACF) and angular velocity (ω-ACF) of the encapsulated H_2O with the electrical intensity of 0.03 V/Å for a representative system, and they are defined as $\langle v(t)\cdot v(0)\rangle$ and $\langle \omega(t)\cdot \omega(0)\rangle$, respectively. The results are plotted in Figure 5. In Figure 5a, the *v*-ACFs of v_x and v_y have similar characteristics with a superposition of a high frequency mode and a low frequency mode that decays much faster. The v_z has a different frequency of oscillation than the v_x and v_y. Besides, it will not approach zero due to the presence of an external electrical field in the *z*-direction. More importantly, compared with the v_x and v_y, the v_z is closest to the *v*-ACF of H_2O@C60, indicating its greatest contribution to the translational motion of H_2O@C60 along *z*-direction motion. The similar results are also obtained in the ω-ACF (Figure 5b). The quick decay in both ω_x and ω_y demonstrates that librations in *x*- and *y*-directions decrease, and ω_z will approach zero eventually, indicating a uniform rotation around the electrical field axis (also agrees well with Figure S6). The quick decay in both ω_x and ω_y demonstrates that the librations around *x*- and *y*-directions decrease, and the energy decrease of librational and rotational motions is expected to transfer to translational motion along *z*-direction, leading to the translational motion of H_2O@C60 along electric field direction. The scarification of rotational energy around *x*- and *y*-direction that gives rise to the translational motion of H_2O@C60 along the electric direction is further confirmed by plotting the angular-velocity cross-autocorrelation function (ω-*v*-ACF) for coupling between the rotational and translational motions (Figure S7).

Since the transport rate of H_2O@C60 depends on θ_0 (Figure 3a), yet it is often desired to control the travel time of the C60 cage-like capsule (e.g. for targeted drug delivery[24]), based on the results in Figures 3 and 4, we propose a strategy to manipulate both the transport direction and rate: after equilibrium of H_2O@C60 in a channel, in spite of its random orientation angle, an pre-electrical field (p*E*) is applied to obtain a steady transport behavior of H_2O@C60 with a constant θ_{ts}^{pE}, and then the particle is temporarily stopped inside the transport channel (e.g. by introducing a switch to "snap" the local nanochannel size below a certain threshold[25]). Through

these two steps, the orientation angle of the encapsulated H_2O molecule has been adjusted to a desired θ_{ts}^{pE}, which depends only on p*E*. Afterwards, a new electrical field (*E*) is applied while the switch is turned off (and the H_2O@C60 is allowed to move axially again), and afterwards the H_2O@C60 will travel at a new steady state (whose rate depends on θ_{ts}^{pE} and *E*, which is controllable).

In summary, we propose a new mechanism for manipulating H_2O@C60 transport by controlling the encapsulated polar H_2O molecule through an external electrical field. Our MD simulations show that, when an external electrical field is applied properly along the axial direction of the channel, steady-state transport of H_2O@C60 can be reached. A strategy is proposed for controlling both the transport direction and rate of H_2O@C60 simultaneously, which may provide useful insights on targeted delivery via C60-like cages.

Acknowledgement

The work is supported by National Science Foundation (CMMI-0643726), DARPA (W91CRB-11-C-0112), National Natural Science Foundation of China (11172231), Changjiang Scholar Program from Ministry of Education of China, and World Class University program through the National Research Foundation of Korea (R32-2008-000-20042-0).

References:

1 M. Saunders, H. A. Jimenez-VAzquez, R. J. Cross, and R. J. Poreda, Science **259**, 1428 (1993).
2 K. Komatsu, M. Murata, and Y. Murata, Science **307**, 238 (2005).
3 G. Liu, A. N. Khlobystov, G. Charalambidis, A. G. Coutsolelos, G. Andrew, D. Briggs, and K. Porfyrakis, J. Am. Chem.Soc. **134**, 1938 (2012).
4 M. Saunders, H. A. Jimenez-Vazquez, R. J. Cross, S. Mroczkowski, M. L. Gross, D. E. Giblin, and R. J. Poreda, J. Am. Chem. Soc **116**, 2193 (1994).
5 Q. Z. T. Pankewitz, S. Liu, W. Klopper, and L. Gan, Angew. Chem. Int. Edn **49**, 9935 (2010).
6 F. Sebastianelli, M. Xu, Z. Bacic, R. Lawler, and N.J.Turro, J. Am. Chem. Soc **132**, 9826 (2010).
7 N. J. Turro, et al., Acc. Chem. Res. **43**, 335 (2010).
8 K. Kurotobi and Y. Murata, Science **333**, 613 (2011).

[9] K. Koga, G. T. Gao, H. Tanaka, and X. C. Zeng, Nature **412**, 802 (2001).
[10] J. Bai, J. Wang, and X. C. Zeng, Proc. Natl. Acad. Sci. USA **103**, 19664 (2006).
[11] G. Hummer, J. G. Rasalah, and J. P. Noworyta, Nature **414**, 188 (2001).
[12] S. Joseph and N. R. Aluru, Nano Lett. **2**, 452 (2008).
[13] C. Dellago, M. M. Naor, and G. Hummer, Phys.Rev.Lett **90**, 105902 (2003).
[14] F. Mikami, K. Matsuda, H. Kataura, and Y. Maniwa, Acs Nano **3**, 1279 (2009).
[15] D. Bucher, Chem. Phys. Lett. **534**, 38 (2012).
[16] H. J. C. Berendsen, J. R. Grigera, and T. P. Straatsma, J. Phys. Chem. **24**, 6269 (1987).
[17] D. Baowan, N. Thamwattana, and J. M. Hill, Phys.Rev.B **76**, 155411 (2007).
[18] M. Y. Amusia and A. S. Baltenkov, Phys. Lett. A **360**, 294 (2006).
[19] R. R. Zope, T. Baruah, M. R. Pederson, and B. I. Dunlap, Phys. Rev. B **77**, 115452 (2008).
[20] S. Plimpton, J. Comput. Phys. **117**, 1 (1995).
[21] B. Xu, Y. Qiao, Y. Li, Q. Zhou, and X. Chen, Appl. Phys. Lett. **98**, 221909 (2011).
[22] J. Li, X. Gong, H. Lu, D. Li, H. Fang, and R. Zhou, Proc. Natl. Acad. Sci. USA **104**, 3687 (2007).
[23] P. G. Kusalik and I. M. Svishchev, Science **265** 1219 (1994).
[24] A. Montellano, T. D. Ros, A. Bianco, and M. Prato, Nanoscale Res Lett **3**, 4035 (2011).
[25] R. Wan, J. Li, H.Lu, and H. Fang, J.Am. Chem. Soc. **127**, 7166 (2005).

Figure Captions:

Figure 1: An electric field is applied along the +*z*-direction of a CNT channel, with electrical intensity E=0.02 V/Å. **(a)** Snapshots of H_2O@C60 transport along the -*z*-direction; **(b)** Axial position transport history of H_2O@C60; note that periodic boundary condition is applied in the axial direction, and thus the H_2O@C60 transports along -z-direction in an infinitely long channel at a steady rate.

Figure 2: **(a)** Schematic of the instantaneous inclined angle (θ_t) between the instantaneous dipolar orientation (p_t) of the encapsulated H_2O and unit vector ($\hat{\mu}$) along the electrical field direction; **(b)** The history of θ_t during the transport of H_2O@C60 under E= 0.02 V/Å.

Figure 3: Effect of the initial inclination angle upon application of electric field (E= 0.02 V/Å), $\theta_0 (=\theta_{t=t_0})$, on the **(a)** history of θ_t and **(b)** axial position transport history of H_2O@C60.

Figure 4: Transport map of H_2O@C60 a CNT channel: region I ($26.7^o < |\theta_{ts}| < 82.6^o$ and 0.006V/Å $< E <$ 0.065V/Å) where the transport is opposite to the electrical field direction (-*z*); region II ($0 \le |\theta_{ts}| \le 26.7^o$ and $E \ge$ 0.065V/Å) where transport is along the direction of electrical field (+*z*); region III ($0 \le E \le$ 0.006V/Å) where the transport direction is unstable.

Figure 5: Autocorrelation functions of **(a)** velocity (*v*-ACF) and **(b)** angular velocity (ω-ACF) of the encapsulated H_2O molecule inside C60 with the electrical intensity of 0.03 V/Å

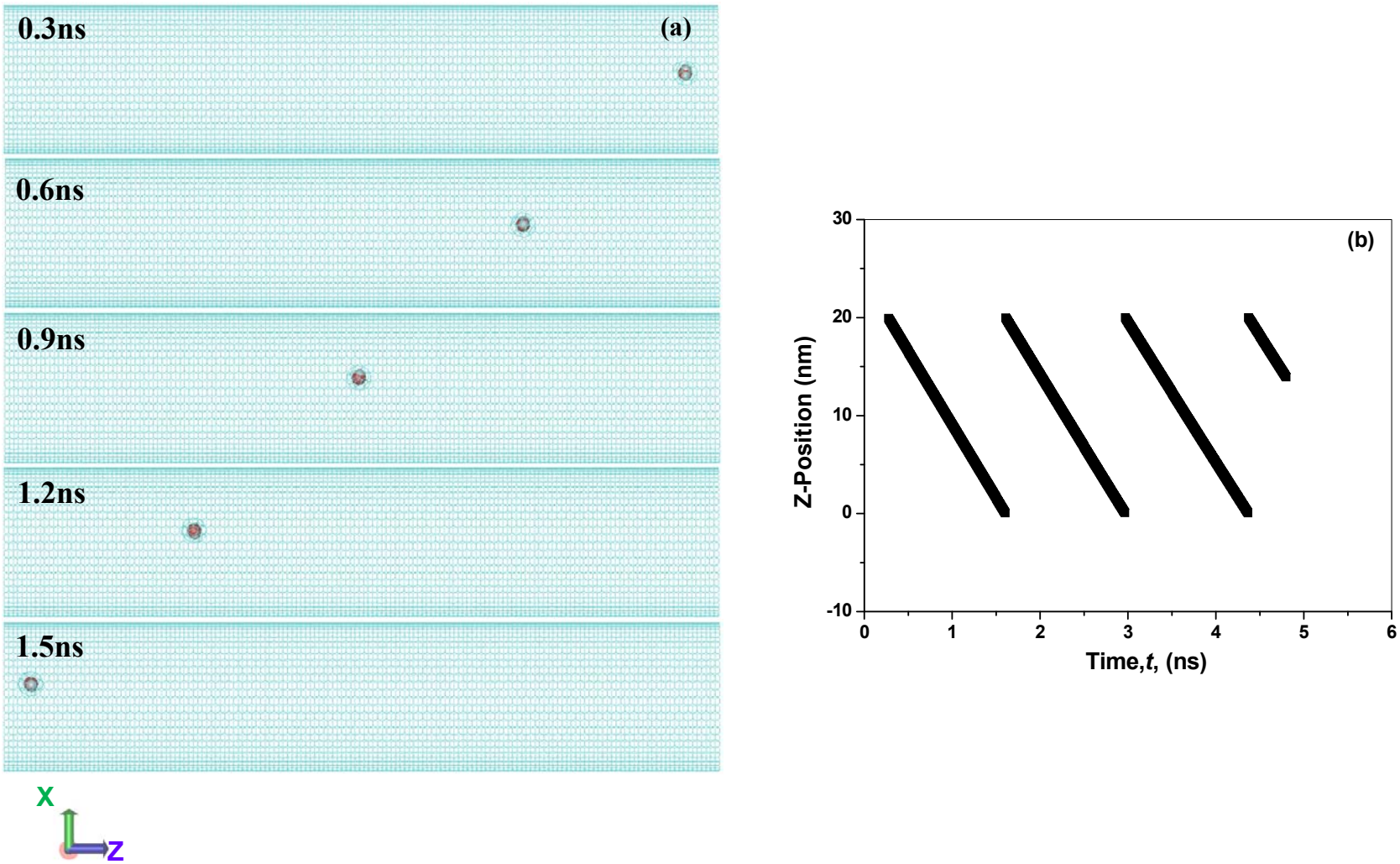

Figure 1: An electric field is applied along the +*z*-direction of a CNT channel, with electrical intensity E=0.02 V/Å. **(a)** Snapshots of H_2O@C60 transport along the -*z*-direction; **(b)** Axial position transport history of H_2O@C60; note that periodic boundary condition is applied in the axial direction, and thus the H_2O@C60 transports along -z-direction in an infinitely long channel at a steady rate.

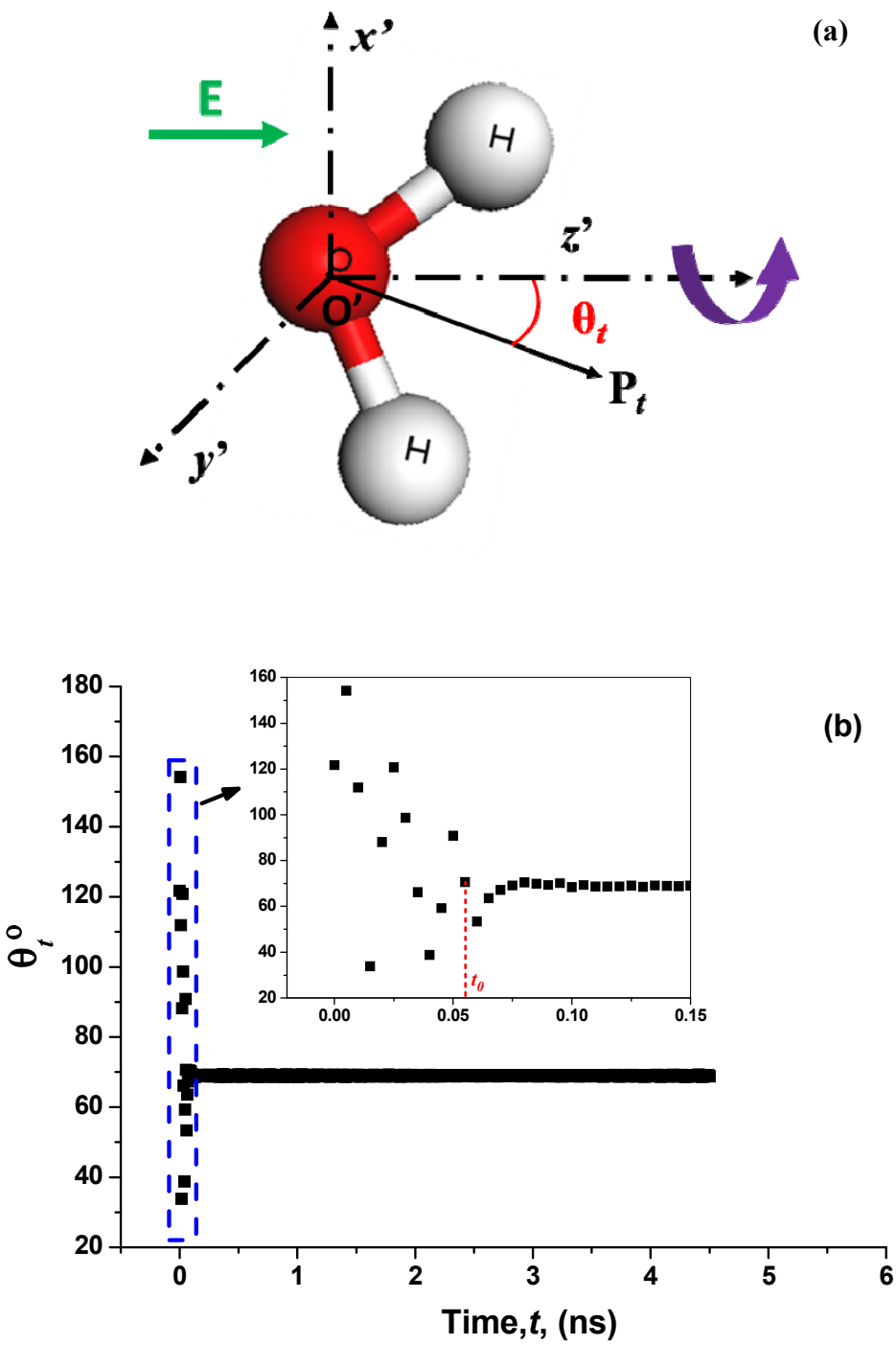

Figure 2: **(a)** Schematic of the instantaneous inclined angle (θ_t) between the instantaneous dipolar orientation (p_t) of the encapsulated H_2O and unit vector ($\hat{\mu}$) along the electrical field direction; **(b)** The history of θ_t during the transport of H_2O@C60 under E= 0.02 V/Å.

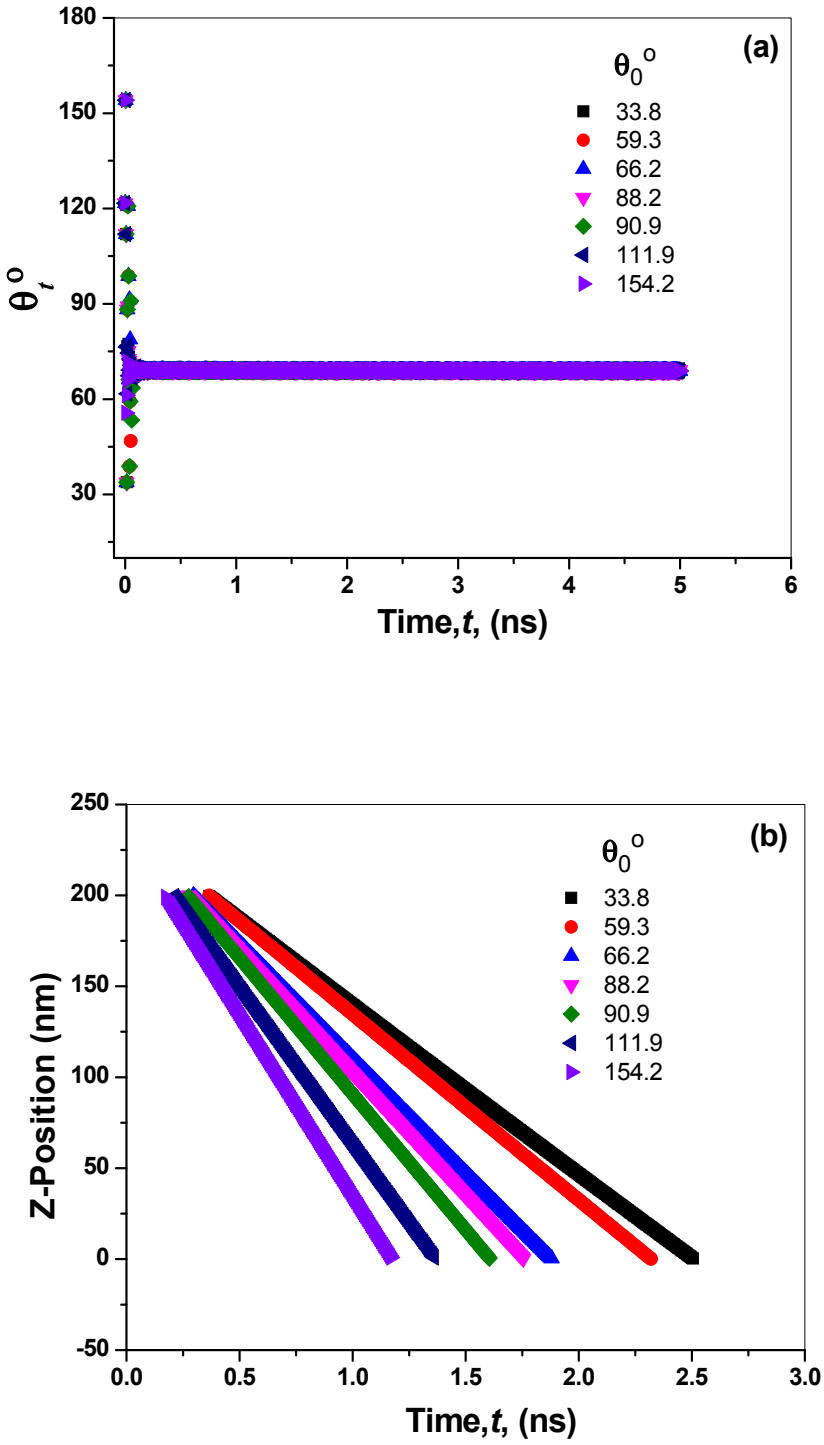

Figure 3: Effect of the initial inclination angle upon application of electric field (E= 0.02 V/Å), $\theta_0 (=\theta_{t=t_0})$, on the **(a)** history of θ_t and **(b)** axial position transport history of H_2O@C60.

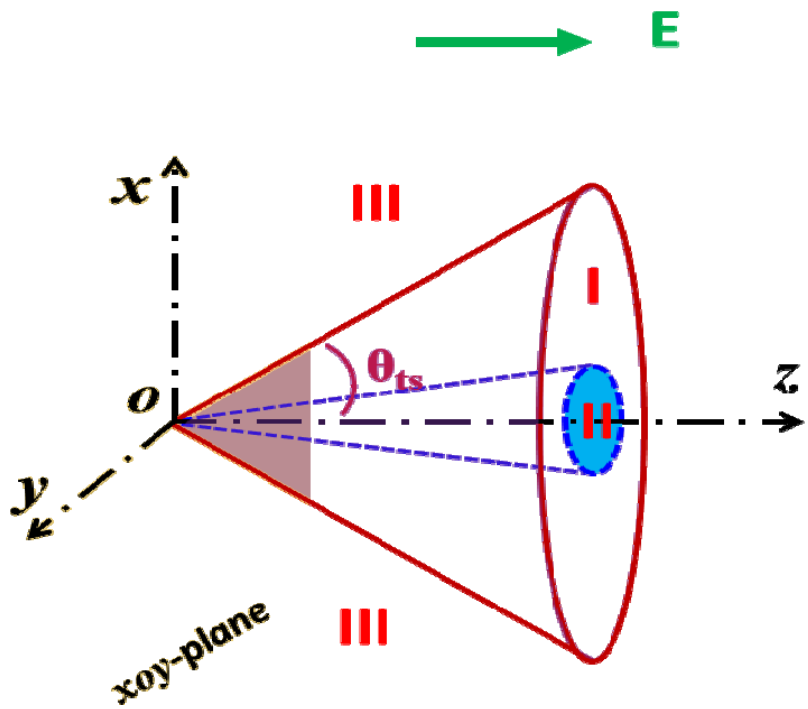

Figure 4: Transport map of H_2O@C60 a CNT channel: region I ($26.7^{o} < |\theta_{ts}| < 82.6^{o}$ and 0.006V/Å $< E <$ 0.065V/Å) where the transport is opposite to the electrical field direction (-*z*); region II ($0 \leq |\theta_{ts}| \leq 26.7^{o}$ and $E \geq$ 0.065V/Å) where transport is along the direction of electrical field (+*z*); region III ($0 \leq E \leq$ 0.006V/Å) where the transport direction is unstable.

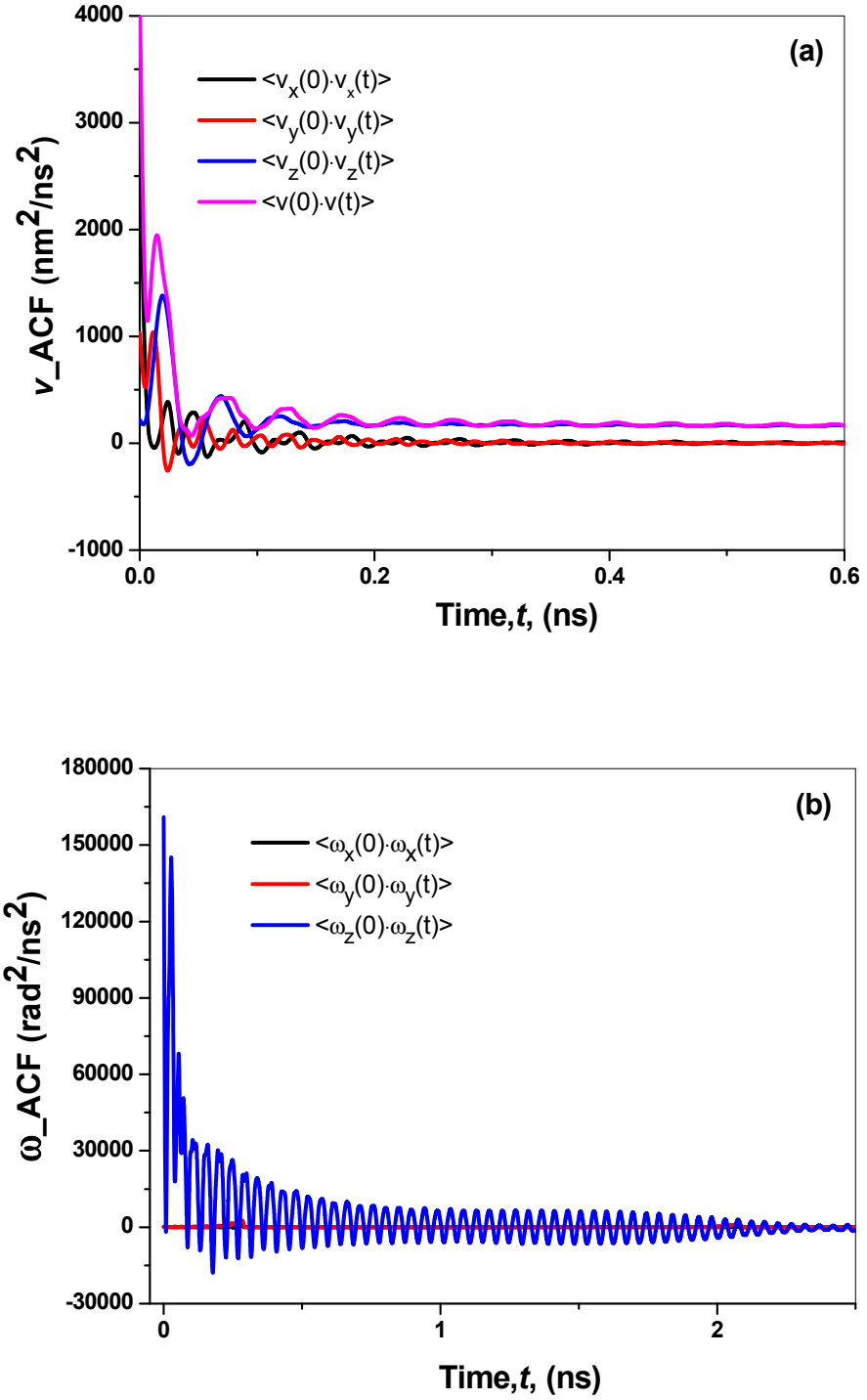

Figure 5: Autocorrelation functions of **(a)** velocity (*v*-ACF) and **(b)** angular velocity (ω-ACF) of the encapsulated H_2O molecule inside C60 with the electrical intensity of 0.03 V/Å.